THE JOURNAL OF PHYSICAL CHEMISTRY B LETTERS

2009, *113,* 9352–9355
Published on Web 06/22/2009

Influence of Nonadiabatic Annealing on the Morphology and Molecular Structure of PEDOT−PSS Films

Antje Schaarschmidt, Abdiaziz A. Farah, Arun Aby, and Amr S. Helmy*

Edward S. Rogers Sr. Department of Electrical and Computer Engineering, University of Toronto, 10 Kings College, Toronto, Ontario, Canada, M5S 3G4

Received: May 04, 2009; Revised Manuscript Received: June 10, 2009

The effect of nonadiabatic annealing on poly(3,4-ethylendioxythiophene)−poly(styrenesulfonate) (PEDOT−PSS) thin films prepared on silicon substrate has been investigated by Raman spectroscopy, X-ray photoelectron spectroscopy (XPS), and atomic force microscopy (AFM). The analysis indicates the formation of an annealing-induced doping in PEDOT structure, suggesting a modification of the polymer electronic structure and the formation of a PEDOT-rich film surface.

Thin film organic semiconducting polymers have been intensively investigated due to their potential for the development of plastic electronic devices.[1] Among these polymers, poly(3,4-ethylenedioxythiophene)−poly(styrenesulfonate) (PEDOT−PSS) has attracted much attention due to its relatively high electrical conductivity, structural stability, transparency in the near-infrared, and low band gap energy.[2] Fabrication processes of organic semiconductor polymers offer advantages over their inorganic counterparts which are used in conventional electronic devices.[3] These advantages include the possibility of using flexible substrates,[4] roll-to-roll manufacturing techniques,[5] and more. However, they are hindered by the low charge mobility, which characterizes transport properties in semiconductor polymers.[6] Significant effort has been aimed at enhancing semiconductor polymer carrier mobilities through the optimization of their structural and molecular order.[7] One of the routes to improve these properties is thermal annealing. It has been demonstrated that the crystalline morphology and the orientation of spin-cast conjugated polymer films could be modestly improved through oven thermal annealing or melt crystallization approaches.[8] These processes are attractive, as they offer a route to control the film properties after casting on the substrate.

The interaction between the polymer and its environment depends in large on the surface composition and structure. Treatments such as vacuum deposition[9] and chemical and plasma processing[10] have been extensively applied to produce surfaces and interfaces of desired characteristics and topologies. The process of rapid thermal annealing (RTA) has been applied extensively in the domain of semiconductor processing and has been demonstrated to assist in enhancing crystallinity and reducing defects in such systems.[11] The benefits offered by this technique have not yet been explored in the field of semiconductor polymers. If successful, RTA can prove to be a pivotal step in controlling certain polymer properties beyond what is achievable using conventional oven-based annealing. In this Letter, we describe the efficacy of the rapid thermal annealing process because of its unique selectivity and short annealing times to influence the morphology and microstructure of PEDOT−PSS thin films. The annealed films were studied using Raman spectroscopy, coupled with X-ray photoelectron spectroscopy (XPS) and atomic force microscopy (AFM).

A PEDOT−PSS aqueous dispersion from Sigma-Aldrich was spin coated onto a precleaned silicon substrate. The samples were then hot baked at 120 °C for 3 min. An average film thickness of 300 nm was determined using ellipsometry. Rapid thermal annealing was performed in an AnnealSys AS-One system. The samples were heated in an inert argon atmosphere up to temperatures ranging between 200 and 300 °C in intervals of 20 °C for a duration of 300 s and with a ramp time of 15 s.

Raman spectroscopy was used first to study the effects of the RTA on the PEDOT−PSS films. Raman spectra were obtained using an HR 800 Horiba Jobin Yvon instrument with a 632 nm excitation wavelength. A Gaussian/Lorentzian fitting routine was applied across the entire spectrum to quantify the peaks. Samples with annealing temperatures above 300 °C were not studied, as the Raman spectra from the polymer samples were degraded such that no peak assignment with any certainty could take place with annealing above 300 °C. This can be attributed to temperature-induced degradation of the interatomic bonding of PEDOT−PSS.[12] The Raman spectrum of the spin coated PEDOT−PSS thin film is shown in Figure 1. The following bands are related to the polymer and are clear in the spectra: 1563 and 1532 cm^{-1} can be assigned to the asymmetric C_α=C_β stretching, 1421 cm^{-1} to symmetric C_α=C_β(−O) stretching, 1365 cm^{-1} to C_β−C_β stretching, 1255 cm^{-1} to C_α−C_α inter-ring stretching, 1093 cm^{-1} to C−O−C deformation, 989 cm^{-1} to oxyethylene ring deformation, 701 cm^{-1} to symmetric C−S−C deformation, 577 cm^{-1} to oxyethylene ring deformation, and 437 cm^{-1} to SO_2 bending. The observed peak positions and their assignment are all in good agreement with published data[13] even though the excitation wavelength is slightly different. This is because the relative peak positions do not change drastically with excitation wavelengths.[14]

Clear differences between the Raman modes of the annealed and unannealed films are evident in the region between 1100 and 1700 cm^{-1}, as depicted in Figure 2A. Peak position shifts

* To whom correspondence should be addressed. E-mail: a.helmy@utoronto.ca.

10.1021/jp904147v CCC: $40.75

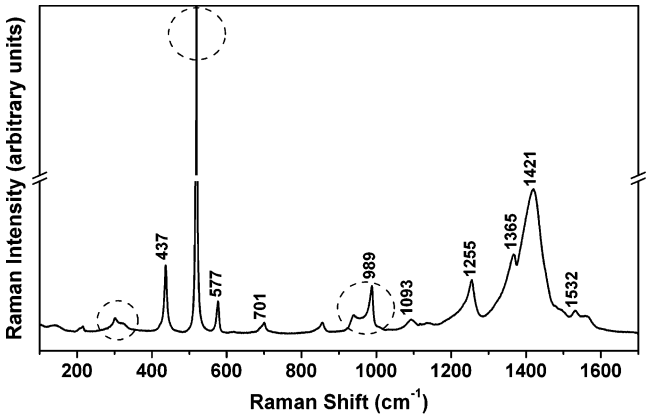

Figure 1. Raman spectra of PEDOT−PSS as-formed film (dotted circles denote silicon substrate vibrations).

and changes in their shape are observed in both the symmetric and asymmetric $C_\alpha{=}C_\beta$ band of the PEDOT. The changes in these bands stem from changes in the electronic structure of the PEDOT chains upon RTA treatment, which favors the materials to become more doped.[15] Notably, the symmetric $C_\alpha{=}C_\beta(-O)$ streching peak at 1421 cm^{-1} for the unannealed sample shifts to a higher wavenumber and reaches 1431 cm^{-1} for the sample annealed at 300 °C. Furthermore, among asymmetric modes, certain peaks become more dominant upon annealing. In particular, the peak at 1495 cm^{-1} increases its relative intensity until it becomes a distinct band in the sample annealed at 300 °C. Other noticeable modes also include peaks at 1532 and 1563 cm^{-1} that are related to asymmetric $C_\alpha{=}C_\beta$ stretching (inset of Figure 2B).[13] The relative peak intensities of these peaks are presumably indicative of some degree of PEDOT polymer chain doping and were analyzed more closely. The integrated intensity ratios of 1495, 1532, and 1563 cm^{-1} for different annealing temperatures are shown in Figure 2B. What can be seen is that, with increased annealing temperature, each of the intensity ratios increases. The resurgence of additional peaks and the shift in the symmetric $C_\alpha{=}C_\beta$ stretching band positions can be utilized to rationalize the induced doped structure of PEDOT herein produced by the RTA. Similar observations were previously reported by Bowmaker et al.[16] where Raman spectroscopy was used to study the level of electrochemical oxidation of PEDOT polymer as reflected by shifts in the positions of several vibrational modes, and particularly the symmetric $C_\alpha{=}C_\beta$ stretching modes. The novelty here is that thermodynamically time stable doped PEDOT structure has been obtained using RTA in inert ambient. Furthermore, the ability of the RTA to control the doping PEDOT films at temperatures where conventional oven annealing has been proven to degrade polymer films is ubiquitously of great technological interest.

X-ray photoelectron spectroscopy (XPS) with a Thermo Scientific Theta Probe spectrometer has also been used to examine the chemical composition of the PEDOT−PSS film before and after annealing. Line shapes and intensities of C 1s, O 1s, and S 2p high-resolution core level spectra were analyzed. The peak fitting of core level C 1s spectra is shown in Figure 3A and B for the unannealed film and the annealed film at 300 °C, respectively. The spectrum for the unannealed film displays three components with binding energies at 284.90, 285.80, and 286.70 eV corresponding to C−C (curve 3), C−C−O (curve 2), and C−S (curve 1) of the PEDOT−PSS, respectively. The C 1s spectra develop some changes in the high-binding-energy side of the main peak representing the C−S and C−C−O with concomitant reduction in intensity of their original peaks for the film annealed at 300 °C. These changes imply that the outermost surface composition of the film becomes rich in alkyl carbons. The changes also suggest that, despite the electronic charge gained by some of these carbon sites, oxygen interdiffusion into the polymer microstructure is not taking place upon annealing. If oxygen interdiffusion was taking place as observed in photothermal degradation of polythiophenes,[17] it could be inferred from either cleavage of the S−C bonds in the thiophene ring or addition of oxygen on the sulfur atom, neither of which were observed by the XPS analysis in any of the films.[18] The sulfur atom in the PEDOT is within the thiophene ring, while the PSS one is presented as a sulfonate moiety. Because of the different sulfur chemical environments, the S 2p electrons of PEDOT and PSS possess different binding energies that can be readily resolved by XPS. The S 2p core level spectra, as shown in Figure 4A, of the unannealed sample and, as shown in Figure 4B, of the 300 °C annealed sample show, as expected, two signature peaks. Each peak involves contributions from a spin-split doublet, S $2p_{3/2}$ and S $2p_{1/2}$, with 1.2 eV energy splitting and 1:2 intensity ratio.[19,20] The S 2p contribution peaks at 163.7 eV (curve 4) and 164.9 eV (curve 3) correspond to sulfur atoms of the PEDOT, and those at higher binding energies at 167.7 eV (curve 2) and 168.9 eV (curve 1) belong to PSS because of the electronegative oxygen attached to the sulfur atom in the sulfonate fragment of the PSS.[18] The intensity of the S 2p contribution from the PEDOT part increases, and that of PSS slightly decreases with increasing the annealing temperature. This observation indicates that the film surface composition changes gradually with the RTA temperature and is turning into a PEDOT accessible surface with increased annealing temperature, contrary to what is expected for PEDOT−PSS interfaces.[2] This property is a pivotal step toward the realization of robust and highly conductive PEDOT−PSS surfaces. Moreover, the line shape and the peak position of the S 2p contribution from the PSS neither change nor shift to a lower binding energy, despite some intensity reduction. This suggests no detachment of oxygen atoms from the sulfonate group and also attests to the integrity of the polymer at the annealing temperatures used, which has not been the case with photolytically annealed semiconducting polymer films.[17] Optical images taken from the same area of preannealed and postannealed films and their corresponding Raman spectra neither change nor reveal any artifacts that may be created during the annealing process (see the Supporting Information).

The O 1s deconvoluted peaks present predominantly three major components at 531.9, 533.2, and 534.3 eV for the unannealed sample, as shown in Figure 4C. A significant difference for oxygen component positions with annealing temperature was observed. The strongest intensities of O 1s in the unannealed sample are observed at 533.2 eV (curve 2) which is assigned to the (C−O−C) component in the PEDOT and 531.9 eV (curve 3) correlating to (O=S) in the PSS.[21] For the 300 °C annealed sample as in Figure 4D, the peak at 531.9 eV (curve 3) remains almost invariant, while the 533.9 eV (curve 2) peak as well as the 535.3 eV peak (curve 1) reduce in intensity and a new peak at 532.8 eV appears. This indicates a different electron charge distribution along the C−O−C bond of the PEDOT resulting from the RTA process. This corroborates the picture of enhanced doping, as suggested by the Raman results. It also agrees with the observation of forming PEDOT accessible surface composition, which is inferred from studying the sulfur XPS data.

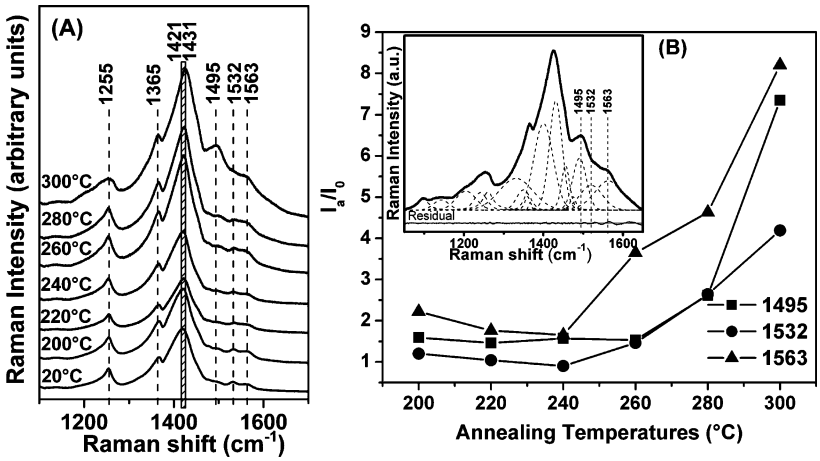

Figure 2. (A) Raman spectra of thermally annealed PEDOT−PSS film in the range of 1100−1700 cm^{-1} at different temperatures. (B) Curve fitting analysis of asymmetric $C_\alpha{=}C_\beta$ stretching vibrations (inset) and their relative ratios of the integrated intensities that results from the annealing process in the range of 1100−1700 cm^{-1}.

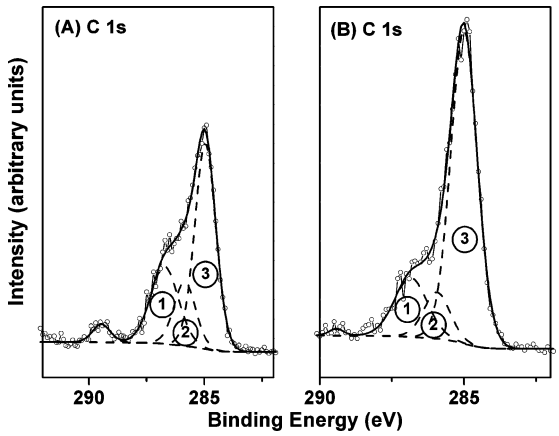

Figure 3. Deconvolution of the C 1s core level of PEDOT−PSS (A) as-formed film and (B) 300 °C thermally annealed film.

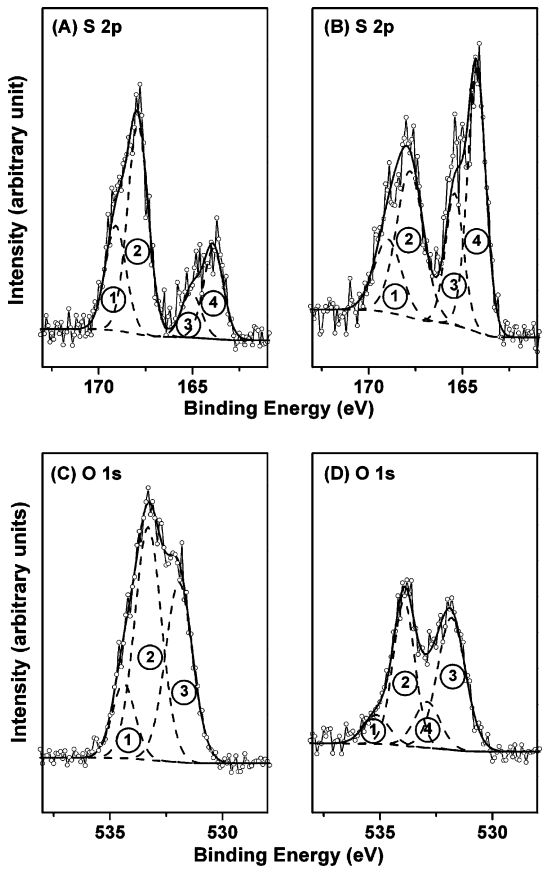

Figure 4. Deconvolution of the S 2p core level of PEDOT−PSS (A) as-formed film and (B) 300 °C thermally annealed film and the O 1s core level of PEDOT−PSS (C) as-formed film and (D) 300 °C thermally annealed film.

The surface morphology of the annealed and unannealed PEDOT−PSS films as well as the bare silicon substrate was imaged using tapping mode AFM. All images were taken from dry surfaces at room temperature in atmosphere. To rule out any image artifacts, trace and retrace AFM scans were compared for consistency among multiple scans. This is to ensure that neither the tip nor the scans altered the surface topology. AFM images of unannealed PEDOT−PSS films and films annealed at 300 °C are shown in Figure 5A and B, respectively. Both images reveal that the film surface is formed of bundles of grain-like structures. Those grains are attributed to phase separated PEDOT−PSS domains surrounded by an excess of PSS chains as expected.[22] The AFM shows flattened bundles in the unannealed samples in comparison to the annealed ones, where surface morphologies with larger granular structures sticking out from the silicon substrate are observed. Film processing parameters could affect the electronic properties of the PEDOT−PSS interface and dramatically change its transport properties.[23] In order to compare the surface roughness of the probe area to the preannealed and postannealed thin films between the probes, the peak heights and root mean square (rms) values were calculated using standard AFM instrument software, as shown in Figures S6, S7, S9, and S10 in the Supporting Information. The peak height for the preannealed PEDOT−PSS film surrounding the probes was 4.72 nm with a rms value of 4.07 nm, while the peak height for the samples annealed at 300 °C was 7.70 nm with a rms value of 6.42 nm. From these AFM analyses, the formation of rough PEDOT chains that spread out onto the planar silicon substrate with increased annealing temperature can be inferred. Furthermore, these results are consistent with previous studies that have demonstrated processing steps that can increase the conductivity of PEDOT−PSS by virtue of rough thin film formation.[23a] The AFM images also corroborate the results obtained from the Raman spectroscopy and XPS, suggesting the formation of highly doped PEDOT polymer chains that could diminish their electrostatic interaction with PSS chains.

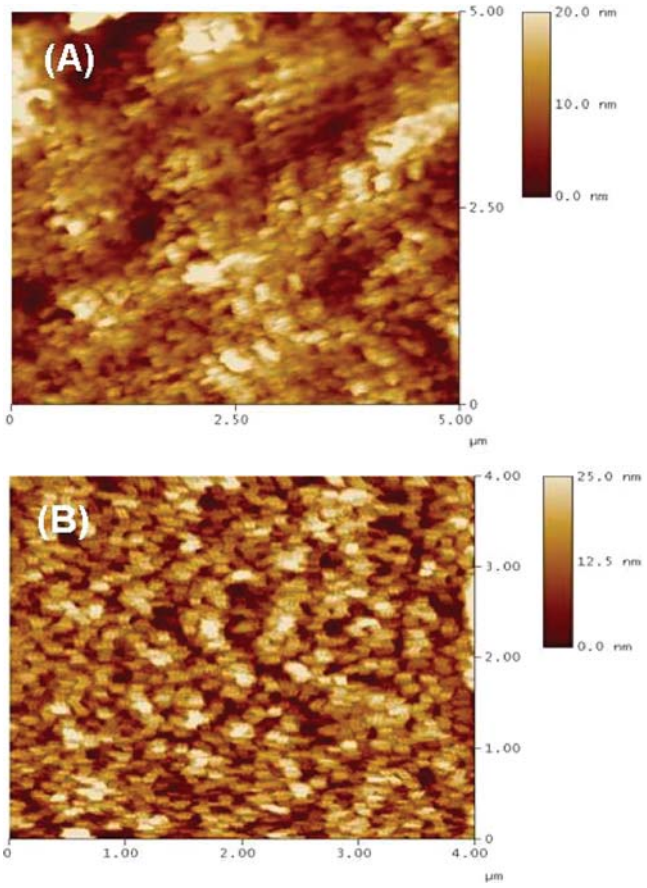

Figure 5. AFM tapping mode height images of PEDOT−PSS (A) as-formed film and (B) 300 °C thermally annealed film.

In conclusion, we have investigated the optical and morphological modifications of PEDOT−PSS thin films on silicon caused by RTA up to 300 °C. Combining the morphological information with the Raman and XPS analyses, an increase in the doping of PEDOT with no indication of oxidative degradation of the film as a function of annealing temperature could be inferred. Since surface composition and topography play a vital role in the performance of semiconducting polymer processing, surface modulating techniques such as RTA can be an important part in the rapid deployment of new materials or better improving the performance of existing materials. As such, we believe that these results present an attractive processing route for further controlling and enhancing the properties of PEDOT−PSS and similar polymer films for device applications.

Acknowledgment. We thank the Surface Interface Ontario at the Chemical Engineering and Applied Chemistry at the University of Toronto Facility for XPS analysis.

Supporting Information Available: Description of the experimental methods and optical images, Raman spectra, cross section analysis, surface roughness analysis, and 3D tapping mode height images of PEDOT−PSS film. This material is available free of charge via the Internet at http://pubs.acs.org.

References and Notes

(1) (a) Allard, S.; Forster, M.; Souharce, B.; Thiem, H.; Scherf, U. *Angew. Chem., Int. Ed.* **2008**, *47*, 4070. (b) Scharber, M. C.; Wuhlbacher, D.; Koppe, M.; Denk, P.; Waldauf, C.; Heeger, A. J.; Brabec, C. L. *Adv. Mater.* **2006**, *18*, 789. (c) Granstrom, M.; Petritsch, K.; Arias, A. C.; Lux, A.; Andersson, M. R.; Friend, R. H. *Nature* **1998**, *395*, 257.

(2) (a) Groenendaal, L. B.; Jonas, F.; Freitag, D.; Pielartzik, H.; Reynolds, J. R. *Adv. Mater.* **2000**, *12*, 481. (b) Kirchmeyer, S.; Reuter, K. *J. Mater. Chem.* **2005**, *15*, 2077.

(3) Reddinger, J. L.; Reynolds, J. R. *Adv. Polym. Sci.* **1999**, *145*, 57.

(4) (a) Kelley, T. W.; Buade, P. F.; Gerlach, C.; Ender, D. W.; Haase, M. A.; Vogel, D. E.; Theiss, S. D. *Chem. Mater.* **2004**, *16*, 4413. (b) Ling, M. M.; Bao, Z. *Chem. Mater.* **2004**, *16*, 4824.

(5) Krebs, F. C. *Sol. Energy Mater. Sol. Cells* **2009**, *93*, 394.

(6) Jaiswal, M.; Menon, R. *Polym. Int.* **2006**, *55*, 1371.

(7) Hoeben, F. J. M.; Jonkheijm, P.; Meijer, E. W.; Schenning, A. P. H. *Chem. Rev.* **2005**, *105*, 1491.

(8) Liu, J.; Guo, T.-F.; Yang, Y. *J. Appl. Phys.* **2002**, *91*, 1595.

(9) (a) Schulz, U.; Kaiser, N. *Prog. Surf. Sci.* **2006**, *81*, 387. (b) Tsujioka, T.; Sesumi, Y.; Takagi, R.; Masui, K.; Yokojima, S.; Uchida, K.; Nakamura, S. *J. Am. Chem. Soc.* **2008**, *130*, 10740.

(10) (a) Chan, K.; Gleason, K. K. *Langmuir* **2005**, *21*, 11773. (b) Tsujioka, T.; Matsui, A. *Appl. Phys. Lett.* **2009**, *94*, 013302.

(11) Singh, R. *J. Appl. Phys.* **1998**, *63*, R59.

(12) Nguyen, T. P.; de Vos, S. A. *Appl. Surf. Sci.* **2004**, *221*, 330.

(13) Garreau, S.; Louarn, G.; Buisson, J. P.; Froyer, G.; Lefrant, S. *Macromolecules* **1999**, *32*, 6807.

(14) Garreau, S.; Duvail, J. L.; Louarn, G. *Synth. Met.* **2002**, *125*, 325.

(15) Lapkowski, M.; Pron, A. *Synth. Met.* **2000**, *110*, 79.

(16) Chiu, W. W.; Travis-Sejdic, J.; Cooney, R. P.; Bowmaker, G. A. *J. Raman Spectrosc.* **2006**, *37*, 1354.

(17) (a) Holdcroft, S. *Macromolecules* **1991**, *24*, 2119. (b) Holdcroft, S. *Macromolecules* **1991**, *24*, 4834. (c) Abdou, M. S. A.; Holdcroft, S. *Macromolecules* **1993**, *26*, 2954.

(18) Crispin, X.; Marciniak, S.; Osikowicz, W.; Zotti, G.; Denier Van Der Gon, A. W.; Louwet, F. C.; Fahlman, M.; Groenendaal, L.; DE Schryver, F.; Salaneck, W. R. *J. Polym. Sci., Part B: Polym. Phys.* **2003**, *41*, 2561.

(19) Castner, D. G.; Hinds, K.; Grainger, D. W. *Langmuir* **1996**, *12*, 5083.

(20) Scofield, J. H. *J. Electron Spectrosc.* **1976**, *8*, 129.

(21) Briggs, D.; Beamson, G. *Anal. Chem.* **1993**, *65*, 1517.

(22) Grecynski, G.; Kugler, T.; Salaneck, W. R. *Thin Film Solids* **1999**, *354*, 129.

(23) (a) Pingree, L. S. C.; Macleod, B. A.; Ginger, D. S. *J. Phys. Chem. C* **2008**, *112*, 7922. (b) Kemerink, M.; Timpanaro, S.; de kok, M. M.; Meulenkamp, E. A.; Touwslager, F. J. *J. Phys. Chem. B* **2004**, *108*, 18820.

JP904147V